

Quantum mechanical coupled channels calculation of the $^{208}\text{Pb} + ^{238}\text{U}(0^+, 2^+, \dots, 40^+)$ reaction

A. J. Baltz

Brookhaven National Laboratory, Upton, New York 11973

(Received 20 May 1988)

Coupled channels calculations are presented for the reaction of 1120 and 1400 MeV ^{208}Pb ions on ^{238}U using a deformed optical model. For scattering angles corresponding to the grazing angle in the 1400 MeV case, the cross-section flux is evenly distributed in a central plateau of final spin states.

There are several reasons for attempting the full quantum-mechanical calculation of the ground-state band inelastic excitation in the reaction $^{208}\text{Pb} + ^{238}\text{U}(0^+, 2^+, \dots, 40^+)$ near the Coulomb barrier. First, as an exercise in computational physics it involves the computation of one of the largest sets of coupled Schrödinger equations that is likely to arise out of a model as simple as the $K=0$ band of the rotational model. Near the upper limit of possible masses for projectiles, Pb excites the strongly deformed ^{238}U to $K=0$ states about as high in spin as would be excited by any other conceivable pair of a target and a projectile. In the calculation I include $K=0$ states up to 40^+ . For partial waves l other than the very lowest, there are $I+1$ subchannels per spin I state. That is, the final orbital angular momentum can take on the values $l-I, l-I+2, \dots, l+I-2, l+I$. Thus, the highest spin state of 40^+ here leads to a total set of 441 coupled Schrödinger equations.

A second point of interest is the reaction mechanism, especially the interplay of the semiclassical and quantum aspects. Of course, this is involved with the computational method as well, since certain approximations, valid in the semiclassical limit, facilitate the partial-wave solution of the coupled Schrödinger equations.¹ However, the relation between the idea of a trajectory and the partial-wave summation actually used in a quantum mechanical solution can also be probed. If the idea of a trajectory is valid anywhere, it should be valid in this case, which has such a large value of the Coulomb parameter, $\eta = Z_1 Z_2 e^2 / v$. And one can investigate how the effect of the nuclear interaction affects the semiclassical aspects.

Finally, there is the interest of the nuclear structure physics. While the highest spin states have been produced by the (heavy ion, Xn) reaction, it still might be of interest to have information from a reaction such as inelastic scattering, where the reaction mechanism is well understood, and as a result information on the parameters of a deformed target can be extracted from the heavy-ion reaction data.

The calculations here reported on were carried out on the Cray 2 at the National Magnetic Fusion Energy (MFE) computer center at Livermore. The fast quantum-mechanical coupled channels code QUICC (Ref. 1) was utilized. A deformed optical model was used with the simple prescription of taking the deformation along

the line joining the center of the ^{208}Pb spherical projectile to the center of the ^{238}U deformed target.

$$U(r, \theta) = \frac{V_0}{1 + e^{-\frac{r - r_{pr} - r_{tr}(\theta)}{a_r}}} + \frac{iW_0}{1 + e^{-\frac{r - r_{pi} - r_{ti}(\theta)}{a_i}}} \quad (1a)$$

$$r_{tr, ti}(\theta) = r_{tr0, ti0} \left[1 + \sum_L \beta_L Y_L^L \right]. \quad (1b)$$

Optical model parameters,² deformation parameters,³ and multipole moments⁴ for Coulomb excitation are taken from the appropriate literature. Angular momentum projections of the deformed optical potential were taken to include $L=0, 2, 4$, and 6 .

$$V_L(r) = 2\pi \int_{\theta=0}^{\pi} \sin\theta d\theta Y_0^L(\theta, 0) U(r, \theta). \quad (2)$$

The elastic scattering potential was taken as the properly normalized $L=0$ projection, and the off-diagonal couplings were taken from the other L projections. Thus, angular momentum states of the target differing by as much as six units of angular momentum are directly coupled to each other.

It is true that a more proper treatment of the geometry would be attained with the folding model⁵ or the deformed proximity model.⁶ In practice such an improved treatment would correspond to an effective nuclear $L=2$ coupling in the present treatment changed by only a few percent and somewhat larger percent changes in the $L=4$ and 6 coupling. Since such changes are at least of the order of present uncertainties in optical potential parameters and would not qualitatively affect the results of the calculations, I follow the center-line prescription for simplicity.

The coupled channels code QUICC (Ref. 1) makes use of a set of coupled first-order equations equivalent to the usual second-order coupled Schrödinger equations. The wave-function solutions in each channel $[ru_i(r) = \chi_i(r)]$ are written in terms of radially varying coefficients, $C_i(r)$, $C_i^+(r)$, of the regular and outgoing $f_i(r)$, $h_i^+(r)$, parts of the homogeneous (uncoupled) wave-function solutions,

$$\chi_i(r) = C_i(r)f_i(r) - C_i^+(r)h_i^+(r).$$

One then immediately obtains from the second-order

coupled Schrödinger equations two sets of coupled first-order equations in $C_i(r)$ and $C_i^+(r)$,

$$\frac{d}{dr} C_i(r) = \frac{1}{k_i} \left[h_i^+(r) \sum_j V_{ij}(r) f_j(r) C_j(r) - h_i^+(r) \sum_j V_{ij}(r) h_j(r) C_j^+(r) \right].$$

$$\frac{d}{dr} C_i^+(r) = \frac{1}{k_i} \left[f_i(r) \sum_j V_{ij}(r) f_j(r) C_j(r) - f_i(r) \sum_j V_{ij}(r) h_j(r) C_j^+(r) \right].$$

The first equation is integrated inward, beginning by ignoring the second term on the right-hand side and using the asymptotic initial condition of only incoming flux in the elastic channel [$C_i(\infty) = -2i\delta_{i0}$] for the first term. Next, the second equation may be integrated outward beginning with the approximate but very adequate physical boundary condition that $C_i^+(r_0) = 0$ for small r_0 . The process is then iterated to convergence.

The variation on the method which I have developed for the Coulomb excitation region is to break the products of homogeneous wave function on the right-hand side into rapidly oscillating and smoothly varying parts. The rapidly oscillating parts may then be discarded in all orders of the iteration, allowing a large step size for the solution in the long-range part.¹ However, in the nuclear interaction and turning point region the equations are solved exactly.

Calculations were carried out for two energies. At 1120 MeV there was little effect of the nuclear optical potential; even for scattering of 180°, 92% of the flux was transmitted. For the 1400-MeV case, however, the nuclear deformed optical potential came fully into play. The quarter point (0.25 of the Rutherford cross section) for the sum of cross sections to all states came at about 104°, and the cross sections were highly absorbed at larger angles. For both cases 10 000 partial waves were included in the Legendre polynomial sum for the final cross sections. However, only 87 were actually calculated for the lower energy case and 65 for the higher. The other scattering amplitudes were then obtained by interpolation for the partial-wave sum.⁷ Fewer partial waves actually had to be calculated for the higher-energy case because of the absorption of the low partial waves which did not occur for the lower energy case.

The strengths of the method used for this problem are that it is iterative and that it allows solutions of the equations in the long-range Coulomb excitation region with a crude step size. Both of these features seem necessary to make the present problem tractable, as will be shown in the following. Solution of the equations was carried out to 400 fm. With the mesh size used in the turning point region (0.01 fm) a brute force second-order Schrödinger equation approach would have required nearly 40 000 radial mesh points. By the technique of keeping only the smoothly varying parts of the effective long-range coupling in the first-order equations, the number of mesh points used was limited to about 500. The number of iterations needed to solve the 441 coupled equations for

each partial wave never exceeded six to achieve an accuracy of one part in 10 000. In contrast, the brute force method would have required 441 independent sets of solutions of the set of 441 coupled equations followed by solving the appropriate set of 441 simultaneous equations for the scattering amplitudes.⁸ The fast methods used al-

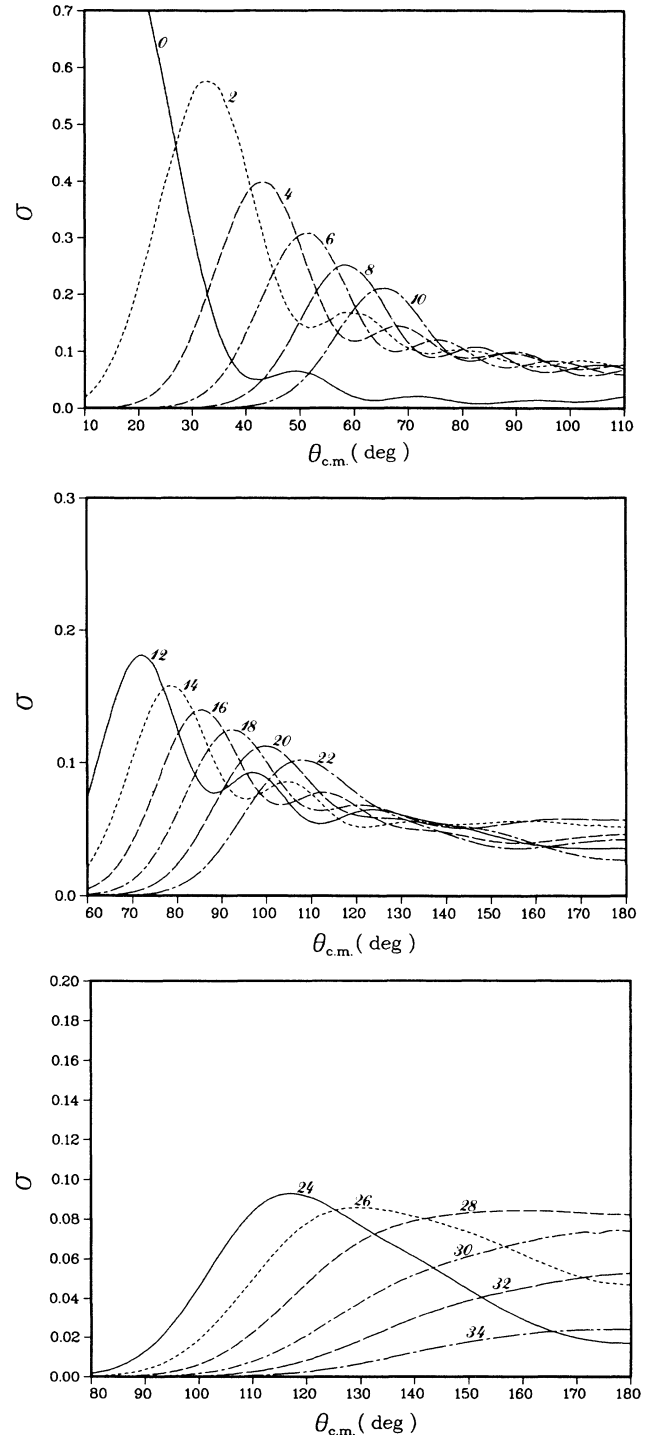


FIG. 1. Angular distributions for $^{208}\text{Pb} + ^{238}\text{U}$ at 1120 MeV. Curves are labeled by the final state of ^{238}U excited in the inelastic reaction. Cross section "sigma" is in units of the ratio to Rutherford scattering.

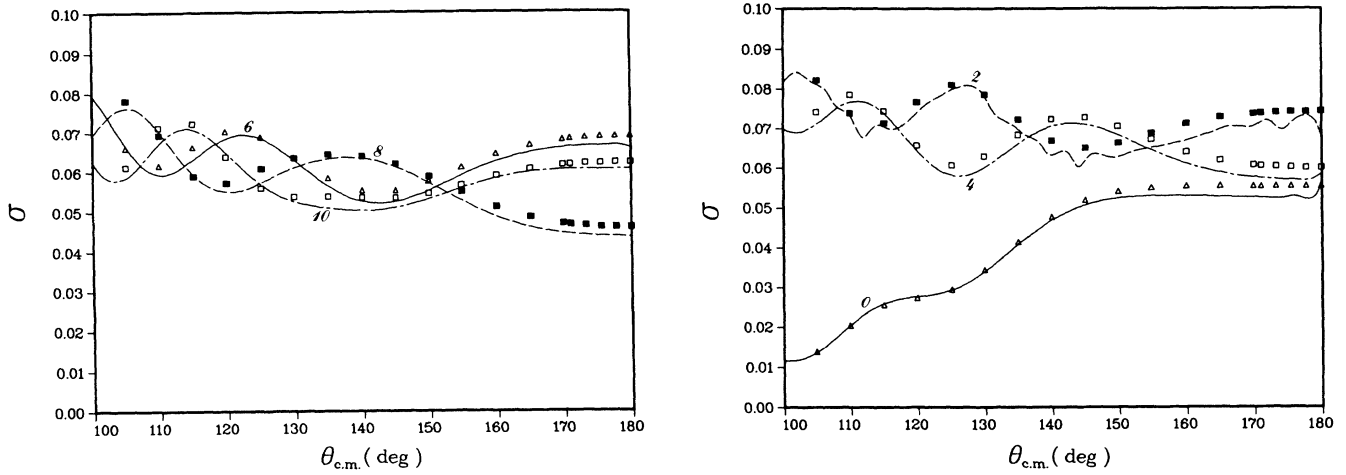


FIG. 2. As in Fig. 1. Angular distributions at 1120 MeV in the backward direction for 0^+ to 10^+ final states. Symbols are cross section values taken from individual partial waves (see text).

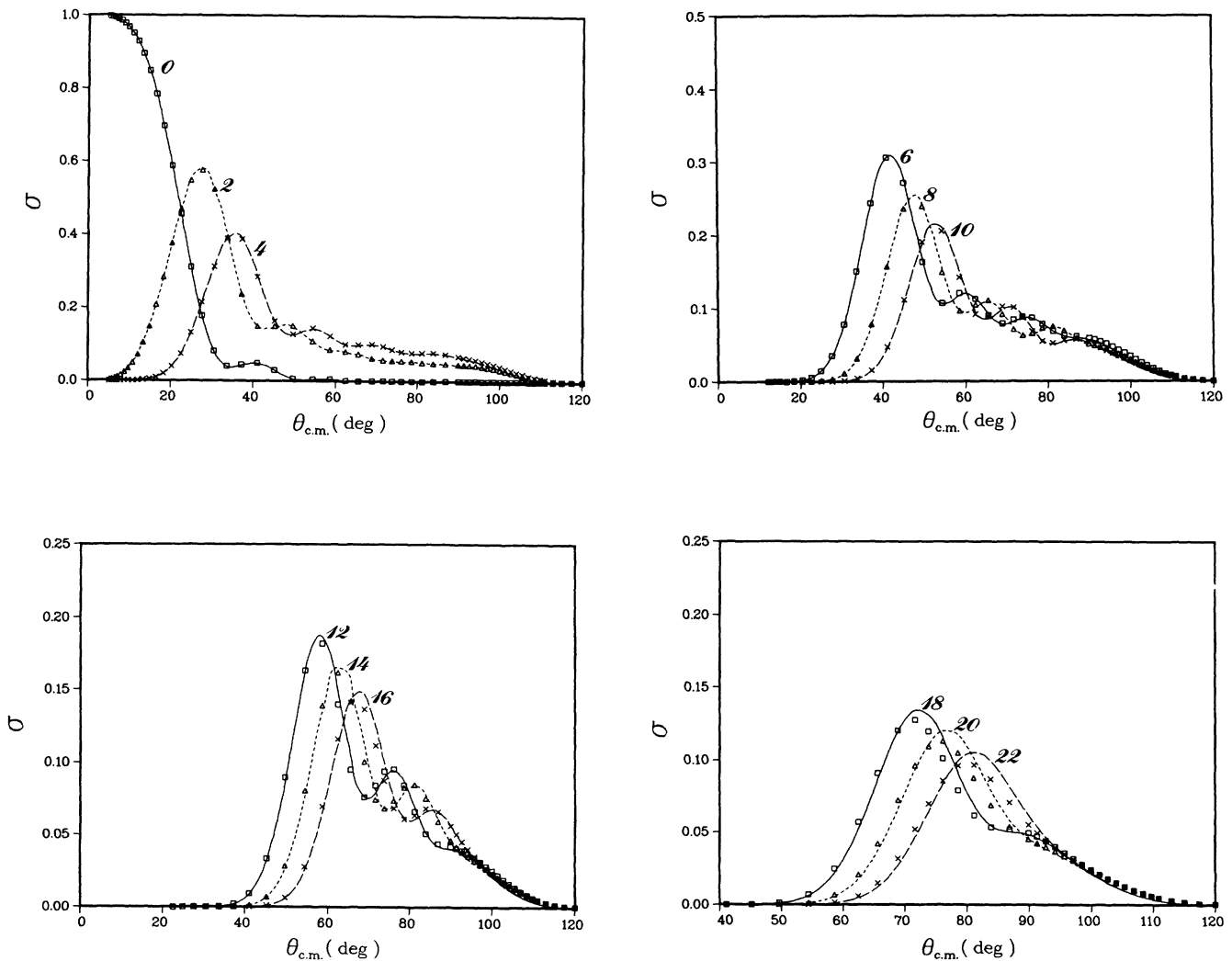


FIG. 3. Angular distributions for $^{208}\text{Pb} + ^{238}\text{U}$ at 1400 MeV. Symbols are cross section values taken from individual partial waves.

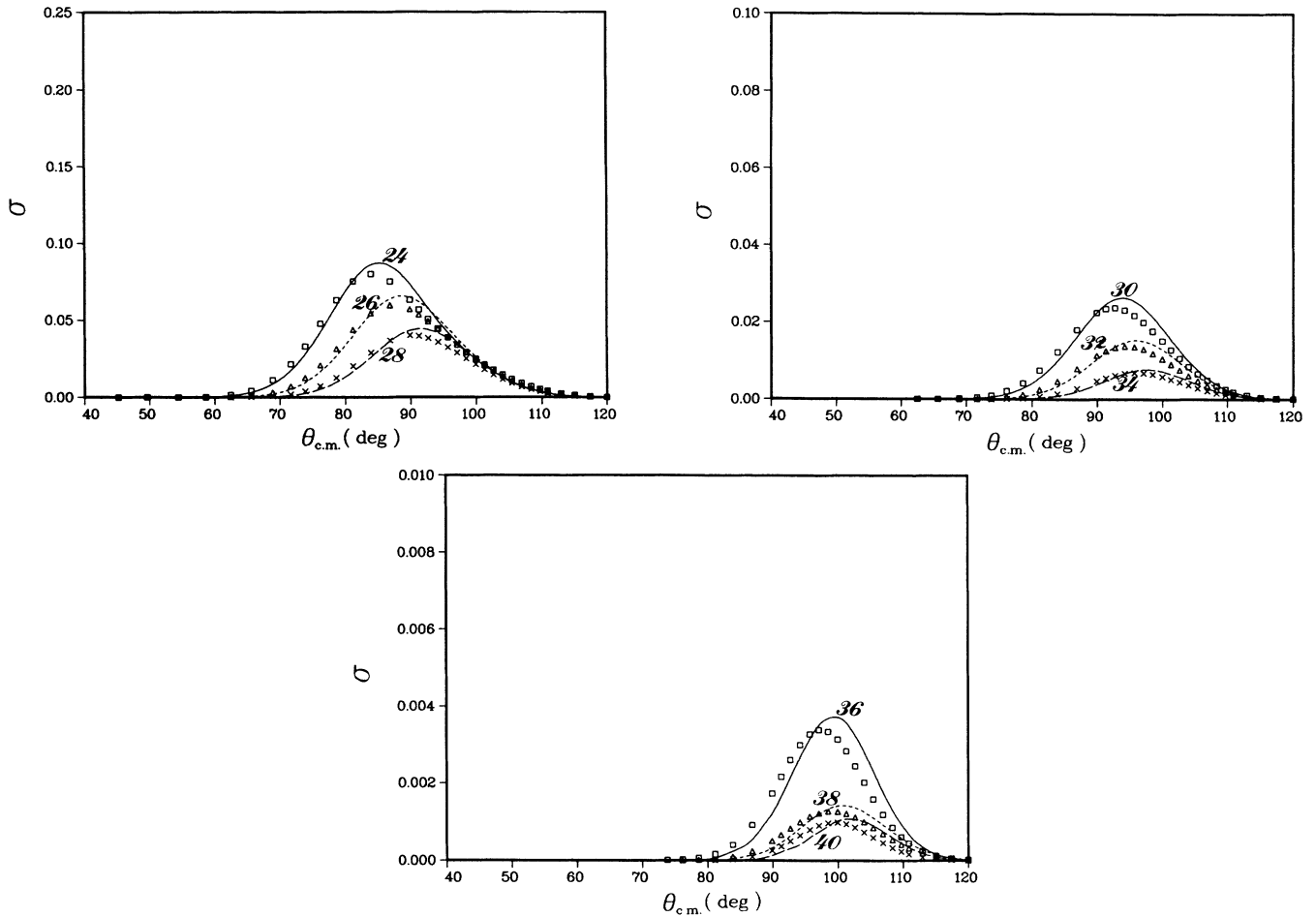


FIG. 3. (Continued).

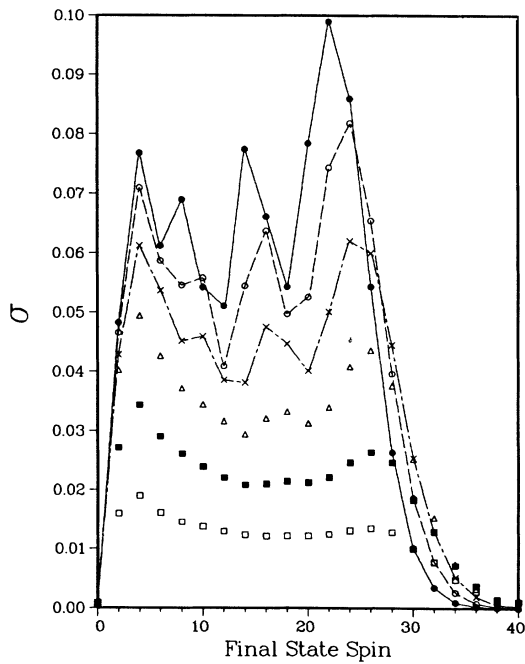


FIG. 4. Cross sections as a function of final spin state at 84° (full circles), 88° (open circles), 92° (crosses), 96° (triangles), 100° (full squares), and 104° (open squares).

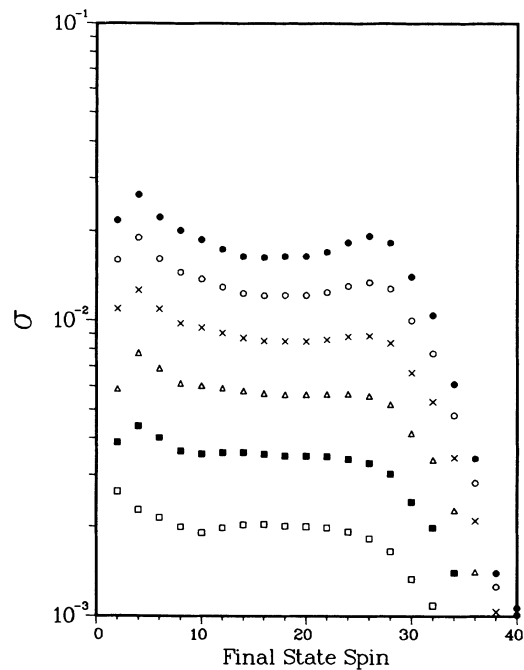


FIG. 5. Cross sections as a function of final spin state at 102° (full circles), 104° (open circles), 106° (crosses), 108° (triangles), 110° (full squares), and 112° (open squares).

lowed a full angular distribution to be calculated in about ten hours on the Cray 2 for each of the two beam energies.

The calculation at 1120 MeV retains the features of Coulomb excitation. In effect, the nuclear interaction is only a relatively small perturbation on the Coulomb excitation, even in the backward direction where its largest effect is to reduce the sum of the cross sections to various final states by no more than 8% from the Rutherford scattering result. The distance of closest approach is 18 fm, corresponding to $r_0 (208^{1/3} + 238^{1/3})$ with r_0 equal to 1.5. Only the tails of the nuclear densities overlap, even at the distance of closest approach.

Angular distributions are shown in Figs. 1 and 2. The usual multiple Coulomb excitation patterns are evident. The lack of smoothness in the backward direction for the cross sections to the ground and first excited inelastic (2^+) state seen in Fig. 2 is no doubt due to the truncation of the partial-wave series at 10 000: even for this high a partial wave, one part in 400 of the scattering flux (cross section) goes into the 2^+ state, indicating the level of inaccuracy of the truncation.

It is interesting to consider the correspondence between the partial wave angular momentum and the scattering angle through the semiclassical relation.

$$\theta = 2 \arctan \left[\frac{\eta}{l + \frac{1}{2}} \right]. \quad (3)$$

We have previously presented a calculation⁹ of the 1120-MeV case at 180° based on this relation by taking the S -matrix elements for each of the final states from the partial wave $l=0$. Since the semiclassical idea of a trajectory certainly has validity here, we may then simply write down the cross section (in units of the Rutherford scattering cross section) as¹⁰

$$\sigma^J(180^\circ) = |S_{l=0}^J|^2 \equiv |C_l^+(\infty) + \delta_{l0}\eta_0|^2$$

where η_0 is the homogeneous scattering amplitude in the elastic channel. We here extend the procedure to higher partial waves and correspondingly more forward angles. In general, the cross section will involve a sum of the squares of the subchannel states allowed for each l coupled to a nonzero orbital angular momentum. Figure 2 also shows cross sections calculated in this one partial-wave semiclassical method as compared to the full Legendre polynomial summation. The symbols indicate all the partial waves actually calculated except in the region of 171° – 180° where only five symbols are shown, corresponding to l of 0, 10, 20, 30, and 40, while actually every low partial wave was calculated. The semiclassical scheme does not show the small bumps at 180° , which we assume arise from the truncation at $l=10\,000$. Using the semiclassical relationship, the $l=10\,000$ partial wave corresponds to a scattering angle of 6° . The sharp truncation reduces the accuracy right around angles of 6° and less, and at 180° .

The situation at 1400 MeV fully involves the nuclear part of the interaction. Here the distance of closest ap-

proach corresponds to an r_0 of 1.2, well into the complex optical potential. Angular distributions are shown in Fig. 3. For the angles forward of about 90° , the calculation shows the usual Coulomb excitation pattern corresponding to trajectories which do not penetrate the nuclear interaction, and for forward angles the semiclassical correspondence between angle and partial wave l [Eq. (3)] holds very well, as is also seen in Fig. 3. A characteristic of this pure Coulomb excitation region is a "picket fence" pattern in the excitation probabilities for the various final states at a given angle. Such a pattern is seen for 84° , full circles (connected by solid lines to guide the eye), in Fig. 4.

It is interesting in Fig. 4 to contrast the situation at 84° which is Coulomb dominated (sum of the flux = 0.92) with that at 104° (open squares), which is near the quarter point in total flux. The effect of the onset of the nuclear interaction with increasing angle is to smooth the distribution of flux between the different final states. A situation is reached in the region of 102° and greater, where there is a broad plateau of final spin states with close to the same cross section (Fig. 5). This broad plateau is in contrast to the analogous physical situation with two nuclei of about half the mass each: 690 MeV $^{134}\text{Xe} + ^{152}\text{Sm}$. In that case,¹¹ with a quarter point at 98° , the cross sections fall smoothly from a maximum at $l=2$ to $l=14$.

What causes the smoothing in Fig. 5 can be understood from Fig. 6. In this figure three cross-section distributions are compared, all of which have a sum equal to about 0.2. The open circles are the 104° distribution seen in Fig. 5. The full circles correspond to the $l=348$ cross section and indicate how a full partial-wave summation is

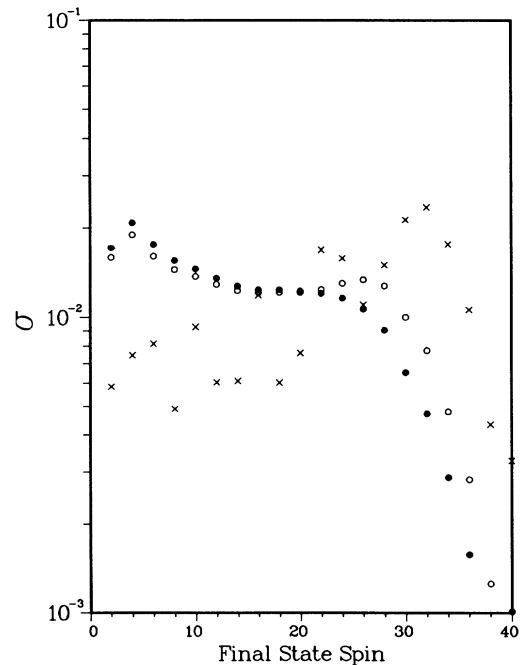


FIG. 6. Comparison of 1400-MeV cross sections whose sum is about 0.2: 104° cross section as in Fig. 5 (open circles), $l=348$ cross section (full circles), and 102° cross section calculated with no off-diagonal nuclear interaction (crosses).

needed in this quarter-point region to obtain the full width of the plateau. But the biggest difference is seen between the cross section, represented by crosses, without the off-diagonal nuclear interaction (but with a spherical complex optical potential) and the cross sections with the off-diagonal nuclear interaction. The smoothing is caused specifically by the off-diagonal part of the complex nuclear optical potential.

In summary, it has been shown that the quantum-mechanical coupled channels method can be successfully implemented in a heavy-ion reaction involving 441 channels and 10 000 partial waves. The general validity of the semiclassical correspondence between orbital angular

momentum and scattering angle has been shown, as well as the utility of a full Legendre polynomial summation for nonforward, non-Coulomb-dominated angles of scattering to obtain the highest level of accuracy. Finally, the onset of the off-diagonal complex nuclear interaction has been shown to lead to a great simplicity in the distribution of cross section among the final states.

I would like to acknowledge useful discussions with J. Weneser. This work was supported by the U.S. Department of Energy under Contract No. DE-AC02-76CH00016.

¹A. J. Baltz, *Phys. Rev. C* **25**, 240 (1982).

²M. W. Guidry, R. W. Kincaid, and R. Donangelo, *Phys. Lett.* **150B**, 265 (1985).

³M. W. Guidry, H. Massmann, R. Donangelo, and J. O. Rasmussen, *Nucl. Phys.* **A274**, 183 (1976).

⁴C. E. Bemis, Jr., F. K. McGowan, J. L. C. Ford, Jr., W. T. Milner, P. H. Stelson, and R. L. Robinson, *Phys. Rev. C* **8**, 1466 (1973).

⁵P. J. Moffa, C. B. Dover, and J. P. Vary, *Phys. Rev. C* **16**, 1857 (1977).

⁶A. J. Baltz and B. F. Bayman, *Phys. Rev. C* **26**, 1969 (1982).

⁷M. Rhoades-Brown, M. H. Macfarlane, and Steven C. Pieper, *Phys. Rev. C* **21**, 2417 (1980); **21**, 2436 (1980).

⁸T. Tamura, Oak Ridge National Laboratory Report No. ORNL-4152, 1967 (unpublished).

⁹A. J. Baltz and L. J. B. Goldfarb, *Phys. Rev. C* **36**, 1807 (1987).

¹⁰M. J. Rhoades-Brown, R. J. Donangelo, M. W. Guidry, and R. E. Neese, *Phys. Rev. C* **24**, 2747 (1981).

¹¹A. J. Baltz and P. D. Bond, *Phys. Lett* **125B**, 25 (1983).